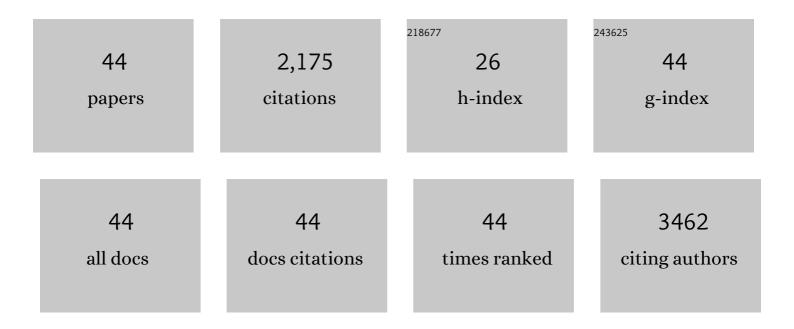
Yi-Ming Yan

List of Publications by Year in descending order

Source: https://exaly.com/author-pdf/1083281/publications.pdf Version: 2024-02-01



YI-MING YAN

#	Article	IF	CITATIONS
1	Ni-doping induced structure distortion of MnO2 for highly efficient Na+ storage. Chemical Engineering Journal, 2022, 429, 132521.	12.7	29
2	Dual-directional electronic modulation of manganese oxides enabled by heterostructures for efficient sodium ion storage. Journal of Power Sources, 2022, 521, 230969.	7.8	5
3	Shearing Sulfur Edges of VS ₂ Electrocatalyst Enhances its Nitrogen Reduction Performance. Small, 2022, 18, e2106939.	10.0	19
4	An ion-accumulating effect in a hollow carbon bowl electrode: understanding the structure-enhanced volumetric desalination capacity and ion transport kinetics in capacitive deionization. Journal of Materials Chemistry A, 2022, 10, 9988-9996.	10.3	15
5	In operando identification of the V ⁴⁺ -site-dependent nitrogen reduction reaction of VS _{<i>x</i>} . Journal of Materials Chemistry A, 2022, 10, 10219-10226.	10.3	11
6	Surface Reconstruction with a Sandwich-like C/Cu/C Catalyst for Selective and Stable CO ₂ Electroreduction. ACS Applied Materials & Interfaces, 2022, 14, 13261-13270.	8.0	14
7	Stabilization of Cu ⁺ via Strong Electronic Interaction for Selective and Stable CO ₂ Electroreduction. Angewandte Chemie, 2022, 134, .	2.0	6
8	Stretching the <i>c</i> -axis of the Mn ₃ O ₄ lattice with broadened ion transfer channels for enhanced Na-ion storage. Journal of Materials Chemistry A, 2021, 9, 23506-23514.	10.3	12
9	Adjusting the Coordination Environment of Mn Enhances Supercapacitor Performance of MnO ₂ . Advanced Energy Materials, 2021, 11, 2101412.	19.5	83
10	Rich bulk oxygen Vacancies-Engineered MnO2 with enhanced charge transfer kinetics for supercapacitor. Chemical Engineering Journal, 2021, 417, 129186.	12.7	83
11	Efficient N ₂ reduction with the VS ₂ electrocatalyst: identifying the active sites and unraveling the reaction pathway. Journal of Materials Chemistry A, 2021, 9, 24985-24992.	10.3	12
12	Enhanced Electrocatalytic Oxidation of Formate via Introducing Surface Reactive Oxygen Species to a CeO ₂ Substrate. ACS Applied Materials & Interfaces, 2021, 13, 51643-51651.	8.0	14
13	Enhanced Electrosorption Ability of Carbon Nanocages as an Advanced Electrode Material for Capacitive Deionization. ACS Applied Materials & amp; Interfaces, 2020, 12, 2180-2190.	8.0	22
14	Cu2+ intercalation activates bulk redox reactions of MnO2 for enhancing capacitive performance. Nano Energy, 2020, 74, 104891.	16.0	54
15	Fluorine Doped Cagelike Carbon Electrocatalyst: An Insight into the Structure-Enhanced CO Selectivity for CO ₂ Reduction at High Overpotential. ACS Nano, 2020, 14, 2014-2023.	14.6	119
16	Carbon nanotubes in-situ cross-linking the activated carbon electrode for high-performance capacitive deionization. Separation and Purification Technology, 2020, 239, 116593.	7.9	35
17	Magnesium oxide anchored into a hollow carbon sphere realizes synergistic adsorption and activation of CO ₂ for electrochemical reduction. Chemical Communications, 2020, 56, 6062-6065.	4.1	6
18	Efficient electrocatalytic reduction of CO2 on CuxO decorated graphene oxides: an insight into the role of multivalent Cu in selectivity and durability. Applied Catalysis B: Environmental, 2019, 259, 118044.	20.2	37

YI-MING YAN

#	Article	IF	CITATIONS
19	Synthesis of ultrathin and hierarchically porous carbon nanosheets based on interlayer-confined inorganic/organic coordination for high performance supercapacitors. Journal of Power Sources, 2019, 414, 383-392.	7.8	39
20	Ultrathinâ€Carbonâ€Layerâ€Protected PtCu Nanoparticles Encapsulated in Carbon Capsules: A Structure Engineering of the Anode Electrocatalyst for Direct Formic Acid Fuel Cells. Particle and Particle Systems Characterization, 2019, 36, 1900100.	2.3	10
21	Role of Ultrathin Carbon Shell in Enhancing the Performance of PtZn Intermetallic Nanoparticles as an Anode Electrocatalyst for Direct Formic Acid Fuel Cells. ChemElectroChem, 2019, 6, 2316-2323.	3.4	16
22	Mold-casting prepared free-standing activated carbon electrodes for capacitive deionization. Carbon, 2019, 149, 627-636.	10.3	32
23	Structural engineering of N/S co-doped carbon material as high-performance electrode for supercapacitors. Electrochimica Acta, 2018, 274, 389-399.	5.2	46
24	Methanesulfonic acid-assisted synthesis of N/S co-doped hierarchically porous carbon for high performance supercapacitors. Journal of Power Sources, 2018, 387, 81-90.	7.8	158
25	Porous and high-strength graphitic carbon/SiC three-dimensional electrode for capacitive deionization and fuel cell applications. Journal of Materials Chemistry A, 2018, 6, 19210-19220.	10.3	16
26	Efficient Capacitive Deionization Using Natural Basswood-Derived, Freestanding, Hierarchically Porous Carbon Electrodes. ACS Applied Materials & Interfaces, 2018, 10, 31260-31270.	8.0	81
27	Organic-inorganic hybrid binder enhances capacitive deionization performance of activated-carbon electrode. Carbon, 2017, 123, 574-582.	10.3	34
28	Synthesis of MoP decorated carbon cloth as a binder-free electrode for hydrogen evolution. RSC Advances, 2016, 6, 68568-68573.	3.6	29
29	Preparation of porous reduced graphene oxide using cellulose acetate for high performance capacitive desalination. RSC Advances, 2016, 6, 70532-70536.	3.6	5
30	A photoelectrochemical methanol fuel cell based on aligned TiO ₂ nanorods decorated graphene photoanode. Chemical Communications, 2016, 52, 2533-2536.	4.1	41
31	Enhanced capacitive deionization performance with carbon electrodes prepared with a modified evaporation casting method. Desalination, 2016, 386, 32-38.	8.2	23
32	Templated-preparation of a three-dimensional molybdenum phosphide sponge as a high performance electrode for hydrogen evolution. Journal of Materials Chemistry A, 2016, 4, 59-66.	10.3	95
33	Response to Comment on <i>Spongeâ€Templated Preparation of High Surface Area Graphene with Ultrahigh Capacitive Deionization Performance</i> . Advanced Functional Materials, 2015, 25, 182-183.	14.9	8
34	A bulky and flexible electrocatalyst for efficient hydrogen evolution based on the growth of MoS2 nanoparticles on carbon nanofiber foam. Journal of Materials Chemistry A, 2015, 3, 5041-5046.	10.3	100
35	Crystal plane-dependent electrocatalytic activity of Co3O4 toward oxygen evolution reaction. Catalysis Communications, 2015, 67, 78-82.	3.3	93
36	A novel electrocatalyst for oxygen evolution reaction based on rational anchoring of cobalt carbonate hydroxide hydrate on multiwall carbon nanotubes. Journal of Power Sources, 2015, 278, 464-472.	7.8	47

YI-MING YAN

#	Article	IF	CITATIONS
37	Diethylenetriamine (DETA)-assisted anchoring of Co ₃ O ₄ nanorods on carbon nanotubes as efficient electrocatalysts for the oxygen evolution reaction. Journal of Materials Chemistry A, 2015, 3, 1761-1768.	10.3	79
38	Composition dependent activity of Cu–Pt nanocrystals for electrochemical reduction of CO ₂ . Chemical Communications, 2015, 51, 1345-1348.	4.1	101
39	Beanpod-shaped Fe–C–N composite as promising ORR catalyst for fuel cells operated in neutral media. Journal of Materials Chemistry A, 2014, 2, 2623.	10.3	49
40	Spongeâ€Templated Preparation of High Surface Area Graphene with Ultrahigh Capacitive Deionization Performance. Advanced Functional Materials, 2014, 24, 3917-3925.	14.9	239
41	Water Treatment: Spongeâ€Templated Preparation of High Surface Area Graphene with Ultrahigh Capacitive Deionization Performance (Adv. Funct. Mater. 25/2014). Advanced Functional Materials, 2014, 24, 3838-3838.	14.9	3
42	A high-performance electrocatalyst for oxygen evolution reactions based on electrochemical post-treatment of ultrathin carbon layer coated cobalt nanoparticles. Chemical Communications, 2014, 50, 13019-13022.	4.1	49
43	Ternary polyaniline–graphene–TiO ₂ hybrid with enhanced activity for visible-light photo-electrocatalytic water oxidation. Journal of Materials Chemistry A, 2014, 2, 1068-1075.	10.3	68
44	Cu ₂ O Decorated with Cocatalyst MoS ₂ for Solar Hydrogen Production with Enhanced Efficiency under Visible Light. Journal of Physical Chemistry C, 2014, 118, 14238-14245.	3.1	138